Amide-Linked C4″-Saccharide Modification of KRN7000 Provides Potent Stimulation of Human Invariant NKT Cells and Anti-Tumor Immunity in a Humanized Mouse Model

Noemi Alejandra Saavedra-Avila, Santosh Keshipeddy, Matthew J. Guberman-Pfeffer, Ayax Pérez-Gallegos, Neeraj K. Saini, Carolina Schäfer, Leandro J. Carreño, José A Gascón, Steven A. Porcelli,* and Amy R. Howell*
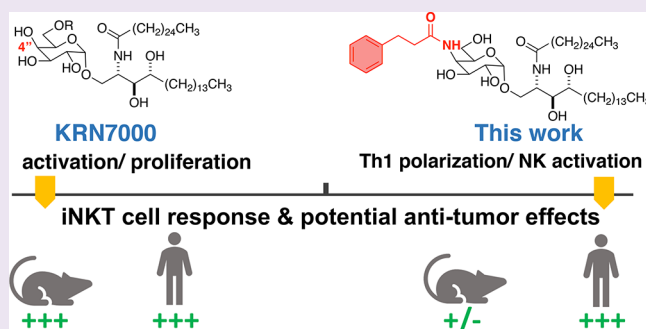
ACCESS | Metrics & More | Article Recommendations | Supporting Information

ABSTRACT: Activation of invariant natural killer T (iNKT) cells by α-galactosylceramides (α-GalCers) stimulates strong immune responses and potent anti-tumor immunity. Numerous modifications of the glycolipid structure have been assessed to derive activating ligands for these T cells with altered and potentially advantageous properties in the induction of immune responses. Here, we synthesized variants of the prototypical α-GalCer, KRN7000, with amide-linked phenyl alkane substitutions on the C4″-position of the galactose ring. We show that these variants have weak iNKT cell stimulating activity in mouse models but substantially greater activity for human iNKT cells. The most active of the C4″-amides in our study showed strong anti-tumor effects in a partially humanized mouse model for iNKT cell responses. *In silico* analysis suggested that the tether length and degree of flexibility of the amide substituent affected the recognition by iNKT cell antigen receptors of the C4″-amide substituted glycolipids in complex with their antigen presenting molecule CD1d. Our findings establish the use of stable C4″-amide linked additions to the sugar moiety for further exploration of the immunological effects of structural modifications of iNKT cell activating glycolipids and highlight the critical need for more accurate animal models to assess these compounds for immunotherapeutic potential in humans.

KRN7000
activation/ proliferation

This work
Th1 polarization/ NK activation

iNKT cell response & potential anti-tumor effects

+++   +++   +/-   +++

INTRODUCTION

Natural killer T (NKT) cells have characteristics of both T lymphocytes and classical natural killer (NK) cells. In contrast to conventional T cells that recognize peptides presented by major histocompatibility complex (MHC) class I or class II proteins, NKT cells recognize glycolipid antigens presented by the MHC class I-like CD1d protein. NKT cells consist of several distinct subsets. The most extensively studied subpopulation, the invariant NKT (iNKT) cells, is characterized by the expression of an invariant TCRα chain (Vα14Jα18 in mice and Vα24Jα18 in humans) paired with a limited range of TCRβ chains. The prototypical iNKT cell antigen is KRN7000 (Figure 1A), an α-galactosylceramide (α-GalCer) derived from structure−activity relationship studies around glycolipids isolated from a marine sponge. Activation of iNKT cells by KRN7000-loaded CD1d elicits immune responses with implications for treating viral and bacterial infections, cancer, and a variety of autoimmune conditions.[1,2] KRN7000 has been investigated in clinical applications, including the treatment of solid and hematological malignancies and viral hepatitis.[3] Key drawbacks of KRN7000 include its stimulation of both T helper 1 (Th1) and Th2

cytokines, which can have opposing effects. It has long been assumed that identifying ligands that selectively elicit Th1 or Th2 cytokines could greatly improve the prospects of developing effective therapeutic applications of iNKT cell activation.[4−6] In addition, the induction of anergy of iNKT cells and hepatic toxicity by KRN7000 have been identified as significant concerns.[7]

Numerous analogs of KRN7000 have been synthesized in an effort to understand structure−activity relationships for iNKT cell glycolipid recognition, and also to produce specific iNKT cell ligands with more favorable activity profiles for potential therapeutic applications.[8] These include variations in the acyl chain and the sphingoid base structures, as well as a variety of changes to the carbohydrate headgroup. For the latter, many active analogs with substitutions at the 6″-position of the sugar
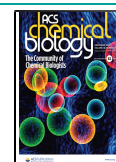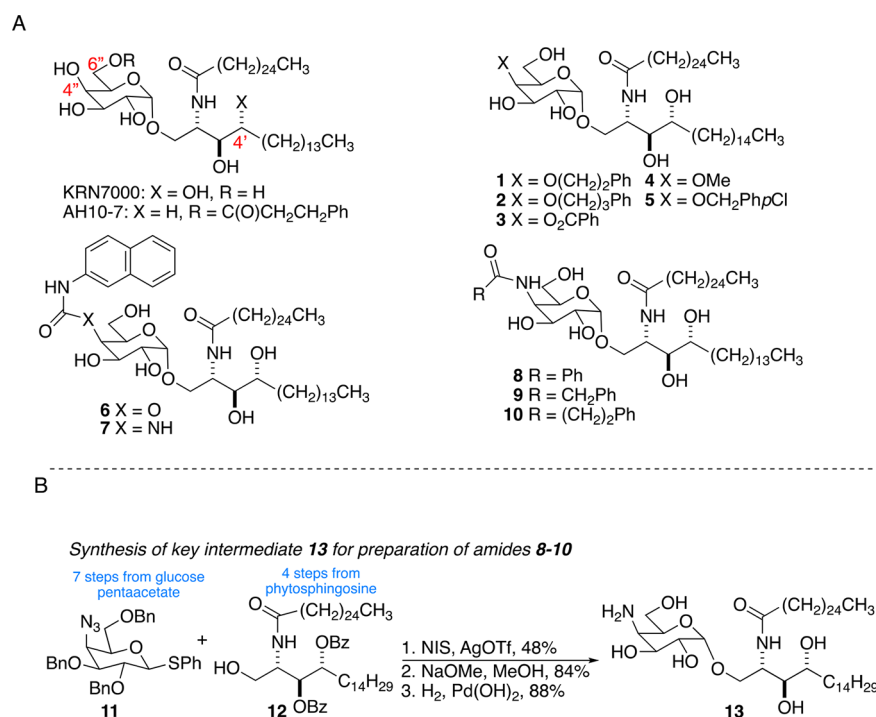
Figure 1. Glycolipid structures and synthesis of C4″ amide linked derivatives of KRN7000. (A) KRN7000 is the prototypical α-GalCer antigen for iNKT cells. AH10−7 is a C6″-modified α-GalCer prepared and evaluated by us previously. Compounds **1−7** are representative C4″-modified KRN7000 derivatives previously described in the literature (see text for references). Amides **8−10** are the focus of this work. (B) Synthetic strategy for the preparation of **8−10**. Each of the amides was prepared by direct acylation of the 4″-amino group of **13**.

(see Figure 1A for numbering) have been described.[6,9−19] Both before and after the structures of binary (glycolipid/CD1d)[20,21] and ternary (glycolipid/CD1d/iNKT cell TCR)[22] complexes were available, studies had shown that the C6″-hydroxyl is not directly involved in interactions critical for iNKT cell stimulation and that this position can be modified with a variety of substituents to enhance potency, alter the balance of cytokine production, and to incorporate fluorescent or biotin labels. The other sugar position that has seen significant exploration of substituents is the C2″ position, where essentially every alteration studied has resulted in inactive compounds.[23,24] This is anticipated from the lipid bound CD1d/NKT TCR ternary structure,[22] which shows that the C2″−OH is involved in hydrogen bond interactions with both CD1d and the T cell receptor, and that it is relatively boxed in by the proteins with little apparent room for accommodating bulkier substitutions. The 3″−OH is also involved in H-bond interactions as a donor to the CD1d protein and potentially also as an H-bond acceptor to the T cell receptor. From the crystal structure there seems to be little room around this position that would allow the introduction of additional atoms, suggesting that this is not likely to accommodate structural modifications. In contrast, the C4″−OH appears not to be essential for stabilizing glycolipid−protein interactions and is positioned in a location that may be more permissive to a range of substitutions.

Initial studies by us and others looked at simple modifications of the C3″- and C4″-positions and concluded that changes at the C3″-position were markedly deleterious to murine iNKT cell stimulation while C4″ substitutions were better tolerated.[24,25] Following the availability of ternary structural data, Wang and co-workers reported C4″-modified analogs containing a limited range of small aliphatic ethers or

acetamide which showed residual iNKT cell stimulating activity.[26] Subsequently bulkier aromatic moieties were incorporated on C4″ via ether or ester linkages (compounds **1−3**, Figure 1A), with a goal of picking up π−π stacking interactions with the iNKT cell TCR.[27] Mouse iNKT cell hybridoma assays showed these compounds to be at least as stimulatory as KRN7000. Mouse *in vivo* cytokine profiles were less clear-cut but did show a marked Th2 bias for **2**. In 2016, Yu and co-workers reported that glucosyl variants of two potent α-GalCer analogs were more potent activators of human iNKT cells than the parent compounds, although they were relatively inactive in mice, thus suggesting significant species variation for alterations at the C4″-position of the glycolipid.[28] Van Calenbergh and co-workers reported a series of C4″-analogs of KRN7000.[29] These included ethers **4** and **5**, carbamate **6**, and urea **7** (Figure 1A). All of the analogs were found to be stimulatory in mice, although not as potent as KRN7000 (with the exception of methyl ether **4**), and all except **4** were Th1 biasing. All of the compounds were able to stimulate human iNKT cells *in vitro*, again with only methyl ether **4** being slightly more antigenic than KRN7000. More recently, based on the polarization of iNKT cell cytokine responses seen with ethers **4** and **5**, van Calenbergh and co-workers prepared an extensive library of 4″-O-alkylated α-GalCers with aromatic and cycloaliphatic moieties with differing tether lengths.[30] None was as potent a stimulus as KRN7000, although several induced a proinflammatory response, suggesting that there could be applications for such compounds as cancer immunotherapeutics or as vaccine adjuvants. Taken together, these results support the hypothesis that modifying the 4″−OH could lead to potent iNKT cell activators that induce biased cytokine responses or other alterations of immunologic functions of iNKT cells.
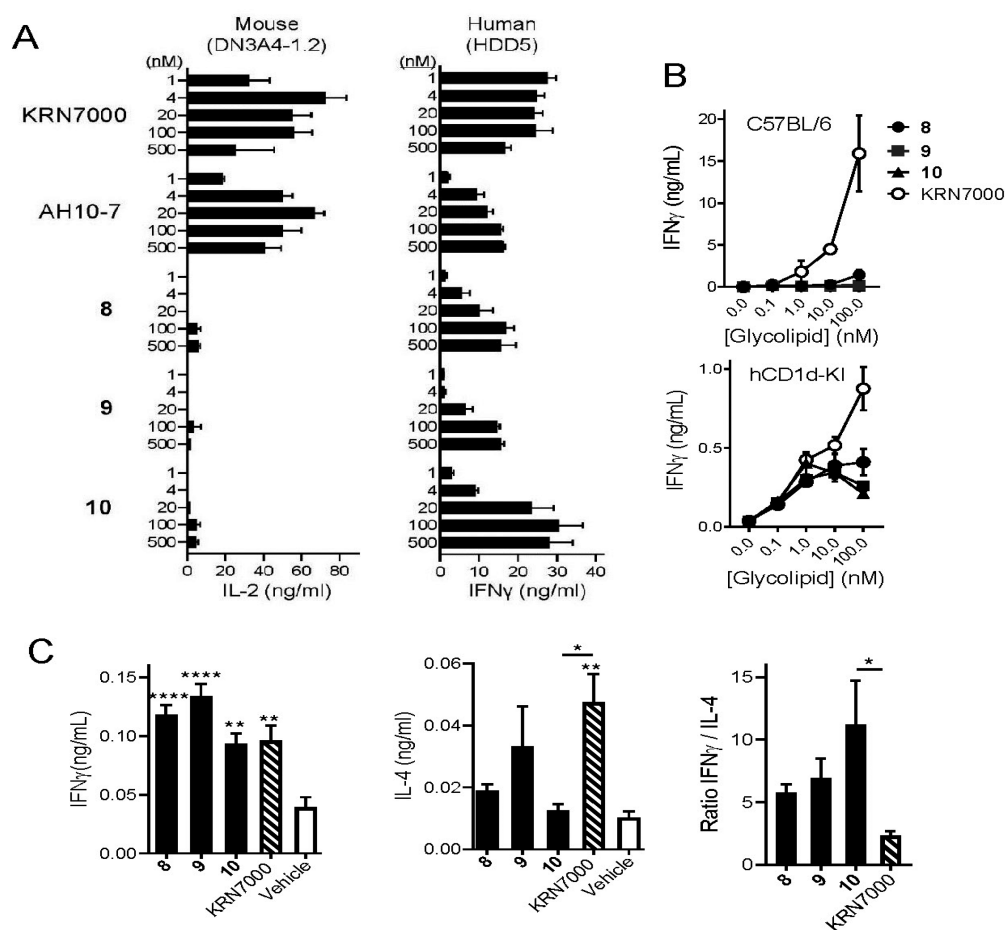
Figure 2. Activation of iNKT cells by C4″ amide variants of KRN7000. (A) Mouse iNKT cell hybridoma DNA3.4−1.2 (left) or human iNKT cell clone HDD5 (right) were stimulated with a range of concentrations of the indicated glycolipids. Mouse iNKT hybridoma cells were cultured with glycolipids plus C57BL/6 strain bone-marrow-derived dendritic cells, and supernatant levels of IL-2 were measured after 24 h. Human iNKT cells were cultured with glycolipids plus HeLa cells transfected to express human CD1d, and supernatant levels of IFNγ were measured after 24 h. Bars show mean values and one standard deviation for triplicate cultures. Results shown are representative of three experiments. (B) Spleen cells from wild type C57BL/6 mice (top) or human CD1d knock-in mice (hCD1d-KI, bottom) were cultured with glycolipids at the concentrations indicated, and supernatant levels of IFNγ at 72 h were determined by ELISA. Symbols show means and error bars represent ±1 SE for triplicate cultures. Results shown are representative of two separate experiments. (C) Serum cytokine levels were determined in hCD1d-KI mice (N = 10 mice per group) following intravenous injection of 4 nanomoles of glycolipids or inert vehicle. Levels of IFNγ at 24 h (left) and of IL-4 at 2 h (center) post injection are shown. The ratio of these values for individual mice was calculated, and the mean values for the groups injected with each glycolipid were calculated (right). Bars represent mean values ±1 SE *$p < 0.05$; **$p < 0.01$; ***$p < 0.001$ for comparisons with vehicle control group, or between **10** and KRN7000 where indicated (ANOVA with Dunnet post-test for multiple comparisons). Results shown are representative of two experiments.

In the current study, we have built on this background work by exploring the effects of amide linked phenyl or phenylalkyl substitutions of the C4″−OH of KRN7000. Although only weakly active in standard mouse models of iNKT cell responses, these compounds showed much greater activities for stimulation of human iNKT cells and in a partially humanized mouse model. The results support further investigation of C4″-modified amide derivatives as potential agents for manipulating iNKT cell responses in humans and emphasize the importance of accurate animal models for assessment of this family of potential therapeutic immunomodulators.

■ RESULTS AND DISCUSSION

Synthesis and Assessment of iNKT Cell Stimulatory Activity of C4″ Modified Glycolipid Amides. Based on examination of the X-ray crystallographic structure of human CD1d and the iNKT cell TCR in complex with KRN7000,[22] our initial goal was to pick up π−π stacking between the glycolipid and the TCR. Our first set of compounds prepared to examine the effect of a phenyl group attached to linkers of different types and lengths was amides **8−10** (Figure 1A). In addition to incorporating an aromatic moiety, the amides could serve as a H-bond donor, acceptor, or both. Although the area directly around the 4″−OH contains polar residues, there is a phenylalanine in what appears to be an accessible hydrophobic region. The approach to the syntheses of the target C4″-modified glycolipid amides **8−10** is illustrated in Figure 1B. The amides were all prepared by direct acylation of fully deprotected amine-containing α-GalCer **13** (Figure 1B). Intermediate **13** was accessed by glycosylation of known disarmed ceramide **12**[31,32] with armed azidothioglycoside **11**,[26] followed by a two stage deprotection involving saponification of the benzoate esters and hydrogenolysis to cleave the benzyl ethers and reduce the azide.

An initial screening for iNKT cell stimulating activity of C4″-modified variants of KRN7000 was carried out with well-established cell culture assays.[33,34] Using interleukin-2 (IL-2) secretion by mouse T cell hybridomas cultured with mouse bone marrow-derived dendritic cells (DCs) as a measure of activation, we found little or no detectable response to the C4″-modified glycolipid amides over a wide range of concentrations. For reference, KRN7000 and the C6″-ester modified glycolipid AH10−7 (see Figure 1A) studied by us previously[19] both gave robust iNKT cell activation over the same range of concentrations (Figure 2A, left). However, when tested with human iNKT cell clones cultured with human CD1d-transfected APCs (Figure 2A, right), the C4″-modified amides showed clear, dose-dependent stimulatory activity, as measured by cytokine secretion (interferon-γ (IFNγ) in this case, since that is the dominant cytokine produced by these human cell lines).[33] Potency for stimulation of human iNKT cell lines (estimated as the concentration required to achieve the maximal response in this assay for a given compound) was comparable to that for AH10−7, and less than for KRN7000, although the peak level for IFNγ with **10** was higher than for the other C4″-amides and comparable to KRN7000. To assess stimulation of primary polyclonal iNKT cells, we cultured mouse spleen cells in the presence of KRN7000 or C4″-amide glycolipids and measured their release of IFNγ into the culture media. With wild type C57BL/6 splenocytes, this recapitulated the findings from mouse iNKT cell hybridomas, showing strong stimulation in response to KRN7000 but undetectable or comparatively weak responses to C4″-amide variants (Figure 2B, top). However, using splenocytes from human CD1d knock in (hCD1d-KI) mice, in which mouse CD1d is replaced by the homologous human protein,[35] we could detect dose dependent responses to all three C4″-amide variants (Figure 2B, bottom).

Overall, these results from *in vitro* assays suggested a moderate level of activity for C4″-amide variants in human or partially humanized mouse iNKT cell stimulation. To analyze this in an *in vivo* setting, we assayed serum cytokine responses in hCD1d-KI mice following a single intravenous injection of glycolipids or inert control vehicle (Figure 2C). Levels of IFNγ were measured in sera obtained at 24 h after stimulation, and IL-4 was measured in sera obtained at 2 h post stimulation, which have been established in previous studies as the time points for peak production of these cytokines.[36] All three C4″-amide variants showed IFNγ production similar in magnitude to KRN7000 in this assay, while showing lower levels of IL-4. This pattern has been previously described as representing iNKT cell activation with a Th1 bias,[19,36] as reflected in the increased ratio of peak levels of IFNγ to IL-4. This ratio trended higher for compounds **8**, **9**, and **10** compared to KRN7000, achieving a significantly higher value relative to KRN7000 for **10** (Figure 2C, right).

Anti-tumor Activity of C4″-Amides. The effects of α-GalCers on stimulating anti-tumor immunity through iNKT cell activation are well documented,[37] and optimizing the structure of glycolipids for this activity remains a major translational goal. As an initial assessment of the anti-tumor activities of C4″-amides **8**, **9**, and **10**, we tested these compounds in comparison to KRN7000 in the B16.F10 model of metastatic melanoma.[35] We used hCD1d-KI mice for these experiments as we have done previously,[19] given their ability to more accurately model the biology of iNKT cell responses in humans.[35] In experiments using a single injection

of glycolipids administered i.v. 3 days after tumor inoculation, we observed a potent anti-tumor effect of C4″-amide compound **10**, which showed suppression of the tumor burden in the lungs that was at least as great as that of KRN7000 and highly significant compared to mice receiving an inert vehicle injection (Figure 3A). The other C4″-amides
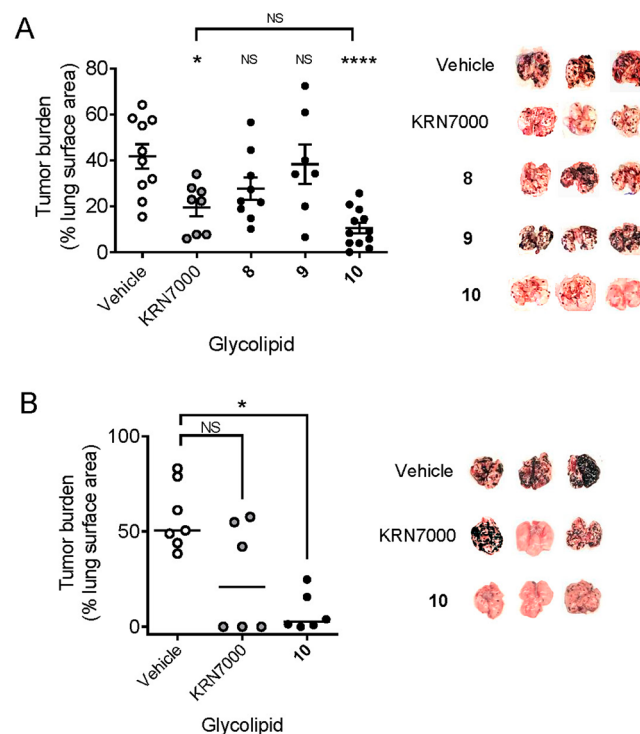

Figure 3. *In vivo* anti-tumor activity of C4″-amide glycolipids. (A) Partially humanized hCD1d-KI mice were injected i.v. with 5×10^5 B16.F10 melanoma cells. Three days later, groups of mice (minimum of 7 per group, range 7−12) received i.v. injections of the indicated glycolipids (4 nmol) or vehicle. Animals were sacrificed 15 days later, lungs were removed, and the percentage of lung surface covered with deeply pigmented metastatic nodules in each animal was determined using ImageJ analysis software. The graph on the left shows individual and median values for mice treated with glycolipids or control (vehicle). Images on the right are representative lungs from three animals in each of the treatment groups. (B) Mice (hCD1d-KI mice, 6−7 per group) were injected i.v. with 5×10^5 B16.F10 melanoma cells, followed by two injections of glycolipids or vehicle administered at day 3 and day 7. Animals were sacrificed 15 days after the second glycolipid injection, lungs were removed and analyzed for tumor burden as in A. Values for individual mice and median values are shown. *$p < 0.05$; ****$p < 0.0001$; NS, not significant (ANOVA with Dunnet post-test for multiple comparisons between glycolipids and vehicle control). The experiment in A was carried out twice with similar results, and the experiment in B has been performed once.

(compounds **8** and **9**) showed no significant anti-tumor activity in this model. A second experiment comparing KRN7000 and **10** directly in this model but using two injections of the glycolipids yielded a similar result with a trend toward superior activity for **10** versus KRN7000, although this did not achieve statistical significance (Figure 3B).

Pronounced Proinflammatory Responses Induced by C4″-Amide Compound 10. To gain insight into the potential mechanisms for the strong anti-tumor effects of compound **10**, we used flow cytometry to directly assess the induction of several important pro-inflammatory molecules by
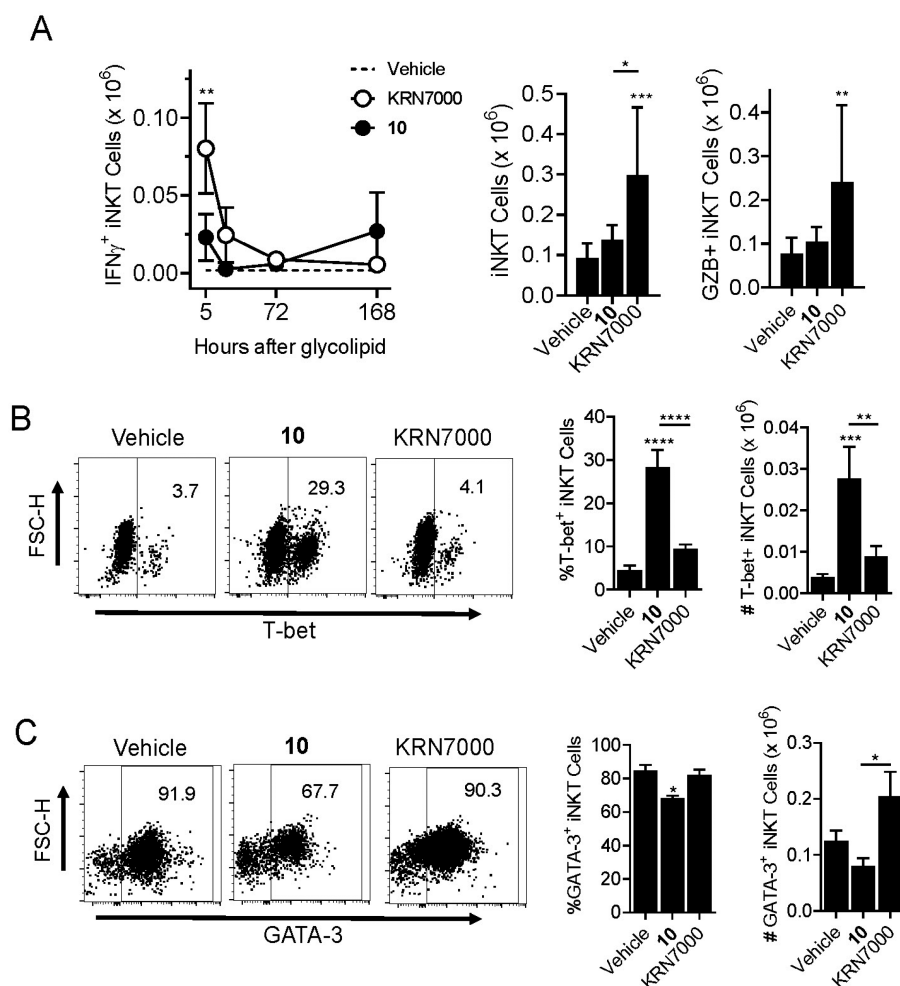
Figure 4. Proinflammatory Th1-biased responses to C4″-amide derivative **10**. Groups of 5 hCD1d-KI mice were injected intravenously with 4 nmol of KRN7000, C4″-amide derivative **10**, or inert control vehicle at 5, 24, 72, or 168 h before they were simultaneously sacrificed. Livers were removed and processed to generate cell suspensions for flow cytometry analysis of cell surface and intracellular markers of iNKT cells, NK cells, and T cells. (A) Analysis gated on KRN7000-loaded CD1d tetramer stained iNKT cells. The graph on the left shows the time course of intracellular IFNγ staining in animals injected with KRN7000 versus compound **10**. Dashed line indicates background staining level in control mice receiving vehicle. Bar graphs show absolute numbers of total iNKT cells (left) and of granzyme B stained iNKT cells (right) at 5 h post glycolipid or vehicle injection. (B) Analysis of intracellular staining of T-bet in gated iNKT cells at 72 h post stimulation with the indicated glycolipid or inert control vehicle. (C) Same as B except showing intracellular staining for GATA-3 in iNKT cells at 24 h post glycolipid or vehicle administration. $*p < 0.05$; $**p < 0.01$; $***p < 0.001$; $****p < 0.0001$ for comparisons to paired values from vehicle treated control mice (ANOVA with Dunnet post-test for multiple comparisons). See Supplemental Figure S1 for details on gating strategy for cell types and analysis of cell surface or intracellular markers.

iNKT cells. Concurrently, we examined these markers on conventional T cells and NK cells, both of which have been shown to be indirectly stimulated following iNKT cell activation, a process referred to as transactivation, which has been linked to proinflammatory and anti-tumor effects of iNKT cells.[33,36] Groups of hCD1d-KI mice were injected once i.v. with either KRN7000, **10**, or inert vehicle and sacrificed at 5, 24, 72, or 168 h post injection. Mononuclear cells were extracted from the livers of these animals, which represent a site of iNKT cell enrichment that facilitates analyses at the single cell level. Cell suspensions were stained with glycolipid-loaded human CD1d tetramers and with antibodies against cell surface and intracellular markers, followed by flow cytometry analysis with selective gating for iNKT cells, NK cells, and conventional T cells (as illustrated in Supplemental Figure S1).

This analysis revealed that IFNγ production by iNKT cells was relatively weak compared to KRN7000 stimulation and was maximal at the earliest time point sampled (5 h).

Expansion of iNKT cells based on absolute counts was also minor or undetectable with **10** in contrast to KRN7000 stimulation, and a similar pattern was observed for granzyme B levels (Figure 4A). However, iNKT cells from animals receiving **10** showed a striking increase in intracellular staining for T-bet, the master transcription factor associated with proinflammatory Th1 polarization of responses (Figure 4B).[38] Conversely, the expression of GATA-3, the master transcription factor opposing Th1 differentiation, was significantly reduced in iNKT cells stimulated with **10** compared to KRN7000 (Figure 4C). A parallel analysis of NK cells and conventional T cells in the same mice revealed enhanced transactivation of these lymphocyte subsets by **10** relative to KRN7000 (Figure 5). This included significantly increased magnitude and prolongation of IFNγ production, as well as significantly increased expansion of granzyme B expression by NK cells in the animals injected with **10** (Figure 5A). Similar
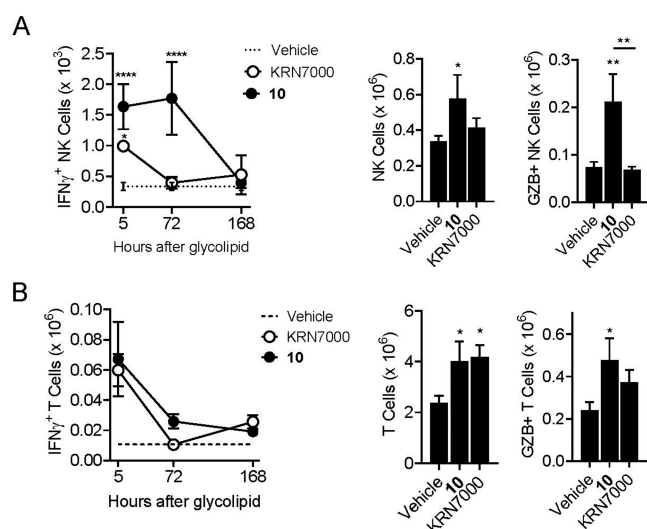
Figure 5. Pronounced transactivation of NK cells and conventional T cells by C4″-amide derivative **10**. Results shown are from analysis of the same mice shown in Figure 4, and graphs are as described in the previous figure. (A) Analysis with gating on NK cells (B220 negative, TCRβ negative, and NK1.1 positive lymphocytes. (B) Analysis with gating on conventional T cells (B220 negative, TCRβ positive, CD1d tetramer negative). *$p < 0.05$; **$p < 0.01$; ***$p < 0.001$; ****$p < 0.0001$ for comparisons to paired values from vehicle treated control mice, or for **10** versus KRN7000 where indicated (ANOVA with Dunnet post-test for multiple comparisons). See Supplemental Figure S1 for details on gating strategy for cell types and analysis of cell surface or intracellular markers.

effects, although less pronounced, were also observed for transactivation of conventional T cells (Figure 5B).

Molecular Modeling of TCR Recognition of C4″-Amides. To understand general features at the level of TCR-ligand recognition that could correlate with the observed biological activities of the C4″-amide derivatives of KRN7000, we performed molecular dynamics (MD) simulations of a fully solvated human CD1d-TCR bound to **8**, **9**, **10**, and KRN7000. Since there is no structural information for a hybrid human CD1D/mouse TCR tertiary complex, we also performed MD simulations of mouse CD1d-TCR bound to those same ligands (see Supporting Information). For each ternary complex, the dynamic nature of protein−ligand interactions was captured using a Simulation Interaction Diagram (SID) to evaluate the occurrence and type of ligand−protein interactions. These results, displayed in Figures 6 and S2, provide percentages that indicate the fraction of time a given residue interacted with the ligand. The most notable difference between **10** and the other amides was that the phenyl group in **10** made no systematic contacts with CD1d or TCR. In contrast, the phenyl moiety interacted with CD1d-His68 via π−π stacking in **8** and π−π stacking with CD1d-Trp153 and TCR-Phe51 in **9** (see also structures in Figure 7). In **8** and **9**, the amide NH group was involved in hydrogen bonds, but this was not the case for **10**. These observations suggested that the alkyl-phenyl group was more flexible and freely positioned in **10** than in **8** and **9**. Analysis of the dihedral angle formed by rotation of the bond adjacent to the amide carbonyl group showed a larger range of angles throughout the MD simulation in **10** compared with the other two compounds (Figure 7, lower panel). Such flexibility was also evident in the visualization of the movement around this bond in the dynamic simulations (see movies included in

Supporting Information). As far as the galactose moiety and the glycosidic linkage, which are common to all ligands including KRN7000, **10** exhibited a more similar set of interactions compared to KRN7000. Among these interactions, the strongest were the two hydrogen bonds with both CD1d-Asp151 and CD1d-Asp80. In contrast, these interactions were less frequent in **8** and **9**. Therefore, it appeared that the greater potency of **10** may be related to having a flexible substituent (i.e., lack of substantial π−π or aromatic hydrogen bond interactions), while retaining a similar set of interactions as KRN7000 for the rest of the glycolipid. Thus, the enhanced tumor protection and Th1 biasing effects of **10** could have resulted from other favorable properties, such as solubility and its uptake or distribution in antigen presenting cells. As we show in the SI, the lack of specific interactions by the phenyl group of **10** is also evident in the MD simulations of mouse CD1D/TCR. Thus, we infer that this lack of interactions would also occur in a hybrid human CD1d/mouse TCR complex.

From a structural point of view, it is unclear why **8**, **9**, and **10** are much less active in standard mouse iNKT cell hybridoma screening assays. From the simulation interaction diagram generated using the mouse CD1d and TCR (see Supplemental Figure S2), we inferred that the type and frequency of the interactions were roughly similar to those found in human CD1d-TCR complexes, with the noteworthy exception that in **8** the galactose adopted a nonstandard orientation that was highly constrained via a cation−π interaction with TCR-Lys68 (Supplemental Figure S3). This highly distorted positioning of the sugar would be anticipated to compromise TCR recognition and may have contributed to the extremely weak responses to compound **8** in fully murine assays. However, our analysis did not predict this conformation to be prominent for murine complexes containing **9** or **10**, and the explanation for their extremely poor stimulatory activity in mice remains unclear.

CONCLUSIONS

In the current study, we synthesized a series of three analog of KRN7000 containing aromatic groups linked with no spacer or by one or two CH_2 groups to the C4″-position via an amide bond. Significantly, we found that, although analogs **8**, **9**, and **10** were only weak activators of mouse iNKT cell responses, these all showed at least moderate potency for human iNKT cell activation in cell cultures, as well as *in vivo* activity for **10** in the human CD1d knock-in mouse model. We were able to take advantage of the partially humanized iNKT cell system of human CD1d knock-in mice to perform detailed investigation of *in vivo* responses, showing pronounced anti-tumor effects that were dependent on the length of the alkane linker and associated with enhanced proinflammatory responses. Overall, our results confirm the notion that the C4″-position of the sugar of an α-GalCer represents a relevant position for structural modification of glycolipid ligands of iNKT cells based on the prototypical KRN7000 structure. In addition, our use of the relatively stable amide linker provides a straightforward approach for linking a variety of substituents to the C4″ of the carbohydrate group.

Several strategies for incorporating substituents on the sugar have yielded varying levels of success in generating active iNKT cell ligands. For example, Zhang et al. concluded that the introduction of aromatic groups on the C4″-position with ether or ester linkers did not block iNKT cell TCR ligand
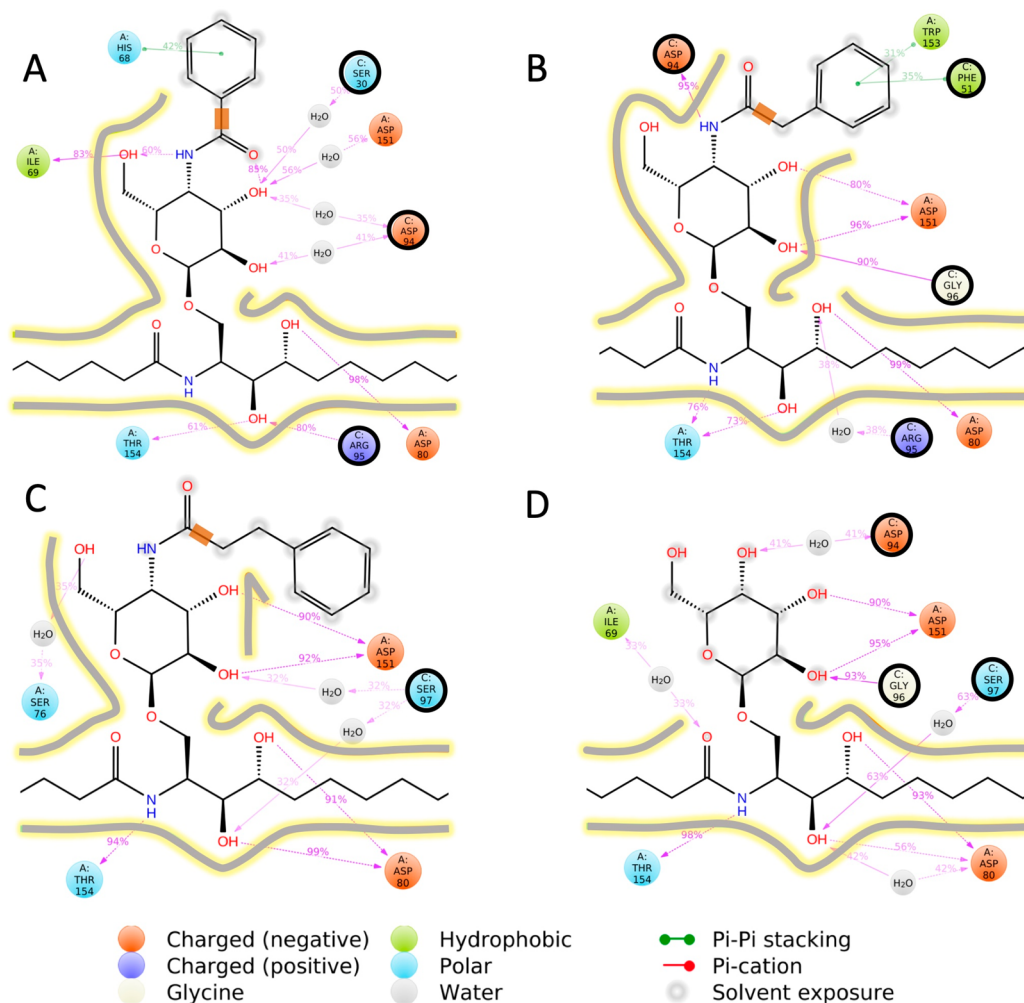
Figure 6. *In silico* analysis of ternary complexes. Molecular dynamics simulation interaction diagrams (SIDs) are shown for the human CD1d-TCR complex containing **8** (A), **9** (B), **10** (C), or KRN7000 (D). Percentages indicate the fraction of time a given residue interacts with the ligand. Only interactions with an occurrence larger than 30% are displayed. The bonds adjacent to the amide's carbonyl group are highlighted as a thick orange line in panels A, B, and C for further discussion in Figure 7. Residues that belong to TCR (chain C) are highlighted with a black circle. Contour lines give an approximation to the protein cavity based on the strength of the ligand−protein interactions.

recognition and in some cases might create analogs with potencies comparable to KRN7000.[27] The group of van Calenbergh reached similar conclusions in their studies of 4″-O-alkylated α-GalCer analogs, initially identifying a C4″-linked p-chlorobenzyl ether as an analog with promising immunostimulating properties, although less potent than KRN7000 based on studies in mice.[29] More recently, they reported synthesis and biologic evaluation in mice of a large panel of 4″-O-alkylated derivatives, concluding that while ether-linked substitutions to the C4″-position decreased the immunogenic potential in mice relative to KRN7000, phenyl modified glycolipids with this structure are able to produce a distinct pro-inflammatory immune response that may be useful for particular applications.[30]

It is important to note that all studies published to date on the biologic activities of C4″-modified α-GalCer analogs have relied mainly or exclusively on analyses using cultured mouse iNKT cells, and *in vivo* evaluation has been limited to standard laboratory mouse strains. In light of the striking species related differences that we observed in the current study, this suggests that past screening efforts have been largely inadequate for characterizing the true biologic activities of C4″-modified

forms of α-GalCer for human iNKT cell responses. Our results indicated that the reduced activity of C4″-amides in assays based on mouse iNKT cells was at least partly reversed by using human CD1d knock-in mice. These animals express human CD1d in place of the endogenous mouse protein and accurately replicate the tissue distribution and levels of iNKT cells that are typical for humans.[19,35] Although the TCRs of iNKT cells in these mice are composed of endogenous mouse TCRα and β chains, they undergo selection for recognition of human CD1d during development, possibly leading also to more human-like receptor structure and specificity. In this model, we found that the C4″-amide glycolipids showed activity both *in vitro* and *in vivo* that was nearly equal to KRN7000 with respect to stimulation of cytokine production.

Significant anti-tumor activity could also be demonstrated for compound **10**, but not for the other two C4″-amides, apparently reflecting a fine-tuning of the overall immune response that depends on subtle variations in the glycolipid structure. It has been suggested previously that appending phenyl substituents to the C4″-position could alter the affinity of TCR interaction with the glycolipid-CD1d complex, either through π−π stacking as suggested by Zhang et al.[27] or
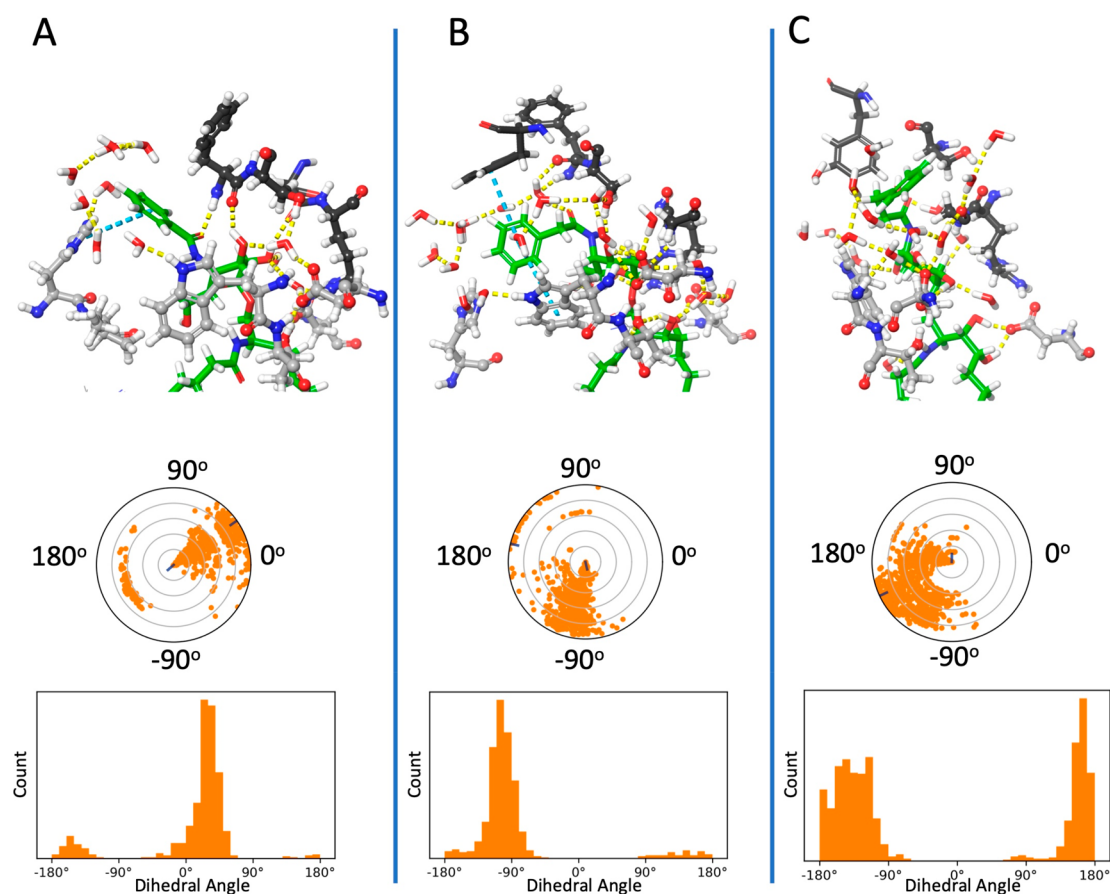
Figure 7. Positioning of glycolipid ligands predicted by molecular dynamics. Representative snapshots are shown from the MD simulation for the human CD1d-TCR complex containing C4″-amide α-GalCer derivatives **8** (A), **9** (B), and **10** (C). Yellow dashed lines indicate hydrogen bonds, and light blue dashed lines indicate $\pi-\pi$ interactions. The C−C bonds of bound glycolipids are colored green, nitrogen atoms are blue, and oxygen atoms are red. Residues of the CD1d and TCR proteins in close apposition to the glycolipid are shown in light gray and dark gray, respectively. Water molecules within 4 Å from the ligand are also displayed. Lower panels show the distribution of the dihedral angles throughout the MD simulation along the bond adjacent to the amide's carbonyl group (highlighted in orange in Figure 6). The broad distribution in **10** indicated larger displacements of the alkyl-phenyl group.

through an extra hydrophobic interaction between the phenyl moiety and the α2-helix of CD1d.[30] However, our modeling and molecular dynamics analysis of ternary complexes containing **8**, **9**, and **10** did not suggest a uniform effect for the phenyl modification in enhancing interactions within the ternary complex. Thus, it appeared that **10**, which in general was the most active of the C4″-amides in the assays applied, did not pick up substantial $\pi-\pi$ or aromatic hydrogen bond interactions, whereas **8** and **9** did. Conversely, molecular dynamics simulations suggested that the most characteristic feature of **10** was the relatively unconstrained movement of the longer C4″ linker and its attached phenyl group. This suggests that enhanced Th1 cytokine bias, sustained transactivation of NK cells, and the associated anti-tumor immunity could be the result of other properties of **10**. It has been previously shown that characteristics, such as the overall solubility of a glycolipid under physiologic conditions or its partitioning into different subcellular compartments, can impact the response elicited by an α-GalCer analog.[19,34,36,39] In other words, a noninteracting aromatic group may confer more favorable immunologic effects than an interacting one in the context of C4″-substituted amides.

■ MATERIALS AND METHODS

Glycolipids, Synthetic Procedures, and Compound Characterization. KRN7000 was obtained from a commercial source (Avanti Polar Lipids). The synthesis of AH10−7 has been previously reported.[19] All chemicals, solvents, and deuterated solvents were purchased from Sigma-Aldrich, Alfa-Aesar, Oakwood Chemicals, or Fisher Scientific and used as received unless noted. Methylene chloride (DCM) was dried over CaH$_2$. Deuterated chloroform (CDCl$_3$) was dried over activated 4 Å molecular sieves. All reactions, unless specified, were conducted under an atmosphere of N$_2$ in glassware that had been oven or flame-dried. ^{1}H NMR spectra were recorded at 400 MHz and/or at 500 MHz and calibrated to the residual CHCl$_3$ peak at 7.27 ppm, the pyridine signal at 8.74 ppm, or TMS at 0.00 ppm. ^{13}C NMR spectra were recorded at 100 MHz and/or at 125 MHz and calibrated to the CDCl$_3$ peak at 77.2 ppm, the pyridine peak at 150.4 ppm, or TMS at 0.0 ppm. Chemical shifts are reported in units of parts per million (ppm). Infrared (IR) spectra were recorded on an FT-IR spectrophotometer and are reported in cm^{-1}. High-resolution mass spectra were obtained on an AccuTOF instrument at the University of Connecticut. Specific rotations $[\alpha]_D$ were obtained on a JASCO P-2000 polarimeter, using the sodium D-line as a source, and the concentration (c) is expressed in grams per 100 mL. Flash chromatography was performed on silica gel, 40 μm and 32−63 flash silica. Thin layer chromatography was performed on silica gel (silica gel 60 F254) glass plates, and the compounds were visualized by UV and/or 5% phosphomolybdic acid in ethanol. Experimental details for the preparation of new compounds and

proton and carbon NMR spectra of purified intermediates and final products are available in the Supporting Information.

Mice. C57BL/6 mice were purchased from Jackson Laboratory, and hCD1dKI mice on a C57BL/6 background[35] were bred and maintained in the animal facilities of the Albert Einstein College of Medicine. Animals were 6−10 weeks of age at the time they were entered into experiments, and only female mice were used. Animals were maintained according to the guidelines of the Association for Assessment and Accreditation of Laboratory Animal Care, and studies involving mice were specifically approved by the Institutional Animal Care and Use Committees (IACUCs) of the Albert Einstein College of Medicine.

Reconstitution of Glycolipids for *in Vitro* and *in Vivo* Use. For *in vitro* assays, glycolipid stock solutions were prepared at 100 mM in DMSO (Sigma). Immediately before use, these stocks were heated to 70 °C, sonicated for 5 min, and then diluted to 1 mM in prewarmed (37 °C) culture medium (RPMI-1640 with 10% FCS). This stock was further diluted with culture medium immediately before adding to cell cultures to give the desired final glycolipid concentrations ranging from 0.01−1000 nM and a final DMSO concentration of 1%. For *in vivo* injection into mice, glycolipids were first dissolved to 20 mM in DMSO and then further diluted to 200 μM using PBS + 0.5% Tween-20. This solution was diluted 1:10 with prewarmed (80 °C) PBS immediately before injection of mice. Injection of 200 μL delivered 4 nmol of glycolipid in a vehicle with a final composition of PBS + 0.1% DMSO + 0.05% Tween-20.

Monoclonal Antibodies and Flow Cytometry. Fluorochrome-conjugated monoclonal antibodies for flow cytometry analyses were obtained from commercial vendors (BD Biosciences except where indicated otherwise) and included the following: anti-GATA-3 (BUV395 conjugate, clone L50−823), anti-NK1,1 (BV605 conjugate, clone PK136), anti-CD4 (BV786 conjugate, clone RM4−5), anti-TCRβ (FITC conjugate, clone H57−597), anti-B220 (APC-Cy7 (conjugate, clone RA3−6B2), anti-Granzyme B (PE-CFS597 conjugate, clone GB11), anti-IFNγ (AF700 conjugate, clone XMG1.2), and anti-T-bet (PE-Cy7 conjugate, clone eBio4B10, from eBiosciences). Human or mouse CD1d tetramers loaded with glycolipid PBS-57 were either APC or PE conjugated and were obtained from the NIH Tetramer Core Facility. Samples were also stained with the Zombie NIR Fixable Viability Kit (Biolegend) to distinguish live versus dead cells. For flow cytometry analyses, samples of cell suspensions were resuspended in PBS and stained with Zombie NIR and subsequently stained with fluorochrome-conjugated mAbs against surface markers diluted to predetermined optimal concentrations in PBS containing 2% fetal bovine serum (FBS) and sodium azide (0.05%; Sigma-Aldrich). For experiments involving staining of intracellular molecules (T-bet, GATA-3, Granzyme B, and intracellular cytokines), cells were fixed using paraformaldehyde (2% in PBS; Electron Microscopy Sciences), permeabilized using Fixation and Factor Staining Buffer (eBiosciences), and stained with the relevant mAb fluorochrome conjugates. Multiparameter FACS analyses were carried out using an Aurora multispectral flow cytometer (Cytek), and data analysis was done using FlowJo software (BD Biosciences).

***In Vitro* and *in Vivo* Activation of iNKT Cells.** A mouse iNKT hybridoma line from C57BL/6 mice (DN3A4−1.2) was stimulated using standard conditions with mouse BMDCs as APCs, and supernatants were harvested after 24 h for determination of levels of IL-2 by capture ELISA.[34] Cloned human iNKT cell line HDD5 was cocultured in 96-well plates at 2×10^4 cells/well with 2×10^4 human CD1d-transfected HeLa cells in 200 μL of RPMI-1640 supplemented with 10% FBS at 37 °C.[40] Glycolipid antigens were added at concentrations ranging from 1 to 500 nM. Supernatants were harvested after 24 h of culture, and concentrations of human IFNγ were measured by capture ELISA as described.[33,34] For stimulation of primary iNKT cells in splenocyte cultures, 10^6 spleen cells from C57BL/6 or hCD1dKI mice were cultured with different glycolipid concentrations for 72 h in culture, and mouse IFNγ was measured by ELISA. For *in vivo* stimulation of iNKT cells, C57BL/6 and hCD1dKI mice were injected i.v. via the retro-orbital plexus with 4 nmol of

glycolipids in vehicle (PBS + 0.05% Tween-20 + 0.1% DMSO). Mice were bled 2 and 24 h later, and serum samples were stored at −80 °C before cytokine measurement by ELISA. For *in vivo* tracking of iNKT, NK, and T cell activation, glycolipids were injected i.v. via retro-orbital plexus, and organs (spleen and liver) were harvested at a range of time intervals from 5 h to 7 days for the preparation of cell suspensions that were analyzed by flow cytometry.

Determination of B16−F10 Melanoma Lung Metastases. B16−F10 metastasis assays were performed as previously described.[19,35] Wild type C57BL/6 mice or C57BL/6-hCD1dKI mice were injected with 5×10^5 B16−F10 (from ATCC Passage 3) in 200 μL of PBS. After 3 days, 4 nmol of glycolipids was administrated. Two weeks after challenge, mice were sacrificed, the lungs removed, and the area of melanized nodules in the lung surface measured with the use of ImageJ software. Results were expressed as a percentage of the total lung surface area that was occupied by melanized tumor.

Modeling and Computational Methods. Compounds **8**, **9**, and **10** were docked into the mCD1d-TCR and hCD1d-TCR complexes from PDB structures 3HE6 and 2PO6, respectively. These receptor complexes were prepared (e.g., H atoms added, protonation and tautomeric states assigned, and H-bond donor/acceptor groups reoriented) using the Protein Preparation application[41] in Maestro version 10.6.014. Structures of glycolipids **8**, **9**, and **10** were prepared by replacing the C4″-hydroxyl of KRN7000 with phenylamides having 0, 1, or 2 carbon spacers between the ipso carbon of the phenyl and the carbonyl carbon of the amide.

Semiflexible docking was performed with standard precision Glide.[42] The galactose and glycosidic linkage were treated flexibly, while torsions along the sphingoid base and fatty acid chains were fixed to the crystallographic values. This docking protocol was previously successful in reproducing the pose for KRN7000 and AH10−7 found in crystallographic ternary complexes.[19] The top 10 docking poses for each substituted structure were conformationally clustered into distinct poses. The overall best-ranked pose for each ligand in the ternary mouse or human complex served as the starting point for molecular dynamics (MD) simulations.

MD simulations were performed with Desmond for all ligands and KRN7000 in both mouse and human CD1d-TCR.[43] The protein was solubilized with the spherical point-charge (SPC) water model within a 10 Å buffer from the protein. This resulted in a total of ∼110 000 atoms (∼30 000 water molecules) for the various models. All simulations were carried out with the NPT relaxation protocol consisting of 100 ps of NVT Brownian dynamics at $T = 10$ K, 12 ps of NVT Berendsen dynamics at $T = 10$ K, and consecutive 500 ps NPT Martyna, Tobias, and Klein (MTK) dynamics at 10, 50, 100, and 200 K. Finally, the production period was performed with 50 ns of NPT MTK dynamics at 310 K with a 2 fs RESPA integrator time step. A total of 1000 snapshots at 310 K were recorded and analyzed for each MD simulation using the Simulation Interaction Diagram (SID) software within the Schrodinger 2019−4 suite.

Statistical Analysis. Data are shown as mean values with error bars representing one standard error (SE). Levels of significance were $P < 0.05$ (*), $P < 0.01$ (**), $P < 0.001$ (***), and $P < 0.0001$ (****). Statistical analyses were done using GraphPad Prism software. Data with multiple groups were analyzed for overall significance using one-way ANOVA, and the level of significance for pairwise comparisons of selected groups was calculated using the Dunnet post-test. Group sizes (N) for individual experiments are defined in the figure legends.

■ ASSOCIATED CONTENT

ⓈI Supporting Information

The Supporting Information is available free of charge at https://pubs.acs.org/doi/10.1021/acschembio.0c00707.

Experimental procedures and methods, characterization data, proton and carbon NMRs, three supplemental figures (PDF)

Molecular dynamics simulation (MPG)

Molecular dynamics simulation (MPG)

Molecular dynamics simulation (MPG)

■ AUTHOR INFORMATION

Corresponding Authors

Amy R. Howell − *Department of Chemistry, The University of Connecticut, Storrs, Connecticut 06269-3060, United States;* ⊙ orcid.org/0000-0003-1958-6411; Email: amy.howell@uconn.edu

Steven A. Porcelli − *Department of Microbiology and Immunology and Department of Medicine, Albert Einstein College of Medicine, Bronx, New York 10461, United States;* Email: steven.porcelli@einsteinmed.org

Authors

Noemi Alejandra Saavedra-Avila − *Department of Microbiology and Immunology, Albert Einstein College of Medicine, Bronx, New York 10461, United States*

Santosh Keshipeddy − *Department of Chemistry, The University of Connecticut, Storrs, Connecticut 06269-3060, United States;* ⊙ orcid.org/0000-0002-9375-2230

Matthew J. Guberman-Pfeffer − *Department of Chemistry, The University of Connecticut, Storrs, Connecticut 06269-3060, United States*

Ayax Pérez-Gallegos − *Department of Pediatrics (Genetic Medicine), Albert Einstein College of Medicine, Bronx, New York 10461, United States*

Neeraj K. Saini − *Department of Microbiology and Immunology, Albert Einstein College of Medicine, Bronx, New York 10461, United States*

Carolina Schäfer − *Millennium Institute on Immunology and Immunotherapy, Programa de Inmunología, Instituto de Ciencias Biomédicas, Facultad de Medicina, Universidad de Chile, Santiago 8380453, Chile*

Leandro J. Carreño − *Millennium Institute on Immunology and Immunotherapy, Programa de Inmunología, Instituto de Ciencias Biomédicas, Facultad de Medicina, Universidad de Chile, Santiago 8380453, Chile*

José A Gascón − *Department of Chemistry, The University of Connecticut, Storrs, Connecticut 06269-3060, United States;* ⊙ orcid.org/0000-0002-4176-9030

Complete contact information is available at:
https://pubs.acs.org/10.1021/acschembio.0c00707

Author Contributions

A.R.H. and S.A.P. conceived of and designed the project. S.K.K. designed and executed the preparation and characterized compounds **8**−**10**. N.A.S.-A., L.C., N.K.S., A.P.-G., and C.S. did *in vitro* culture, *in vivo* mouse experiments, and flow cytometry. J.A.G. and M.J.G.-P. carried out *in silico* structural analyses. A.R.H., S.A.P., J.A.G., N.A.S.-A., and S.K.K. wrote the manuscript and Supporting Information. All authors have given approval to the final version of the manuscript.

Notes

The authors declare no competing financial interest.

■ REFERENCES

(1) Brennan, P. J., Brigl, M., and Brenner, M. B. (2013) Invariant natural killer T cells: an innate activation scheme linked to diverse effector functions. *Nat. Rev. Immunol.* 13, 101−117.

(2) Carreno, L. J., Saavedra-Avila, N. A., and Porcelli, S. A. (2016) Synthetic glycolipid activators of natural killer T cells as immunotherapeutic agents. *Clin. Transl. Immunol.* 5, e69.

(3) Nair, S., and Dhodapkar, M. V. (2017) Natural killer T cells in cancer immunotherapy. *Front. Immunol.* 8, 1178.

(4) Yu, K. O. A., Im, J. S., Molano, A., Dutronc, Y., Illarionov, P. A., Forestier, C., Fujiwara, N., Arias, I., Miyake, S., Yamamura, T., Chang, Y.-T., Besra, G. S., and Porcelli, S. A. (2005) Modulation of CD1d-restricted NKT cell responses by using N-acyl variants of α-galactosylceramides. *Proc. Natl. Acad. Sci. U. S. A.* 102, 3383−3388.

(5) Miyamoto, K., Miyake, S., and Yamamura, T. (2001) A synthetic glycolipid prevents autoimmune encephalomyelitis by inducing TH2 bias of natural killer T cells. *Nature* 413, 531−534.

(6) Li, X., Chen, G., Garcia-Navarro, R., Franck, R. W., and Tsuji, M. (2009) Identification of C-glycoside analogues that display a potent biological activity against murine and human invariant natural killer T cells. *Immunology* 127, 216−225.

(7) Parekh, V. V., Wilson, M. T., Olivares-Villagomez, D., Singh, A. K., Wu, L., Wang, C. R., Joyce, S., and Van Kaer, L. (2005) Glycolipid antigen induces long-term natural killer T cell anergy in mice. *J. Clin. Invest.* 115, 2572−2583.

(8) Laurent, X., Bertin, B., Renault, N., Farce, A., Speca, S., Milhomme, O., Millet, R., Desreumaux, P., Henon, E., and Chavatte, P. (2014) Switching invariant natural killer T (iNKT) cell response from anticancerous to anti-inflammatory effect: molecular bases. *J. Med. Chem.* 57, 5489−5508.

(9) Guillaume, J., Seki, T., Decruy, T., Venken, K., Elewaut, D., Tsuji, M., and Van Calenbergh, S. (2017) Synthesis of C6″-modified α-C-GalCer analogues as mouse and human iNKT cell agonists. *Org. Biomol. Chem.* 15, 2217−2225.

(10) Pauwels, N., Aspeslagh, S., Elewaut, D., and Van Calenbergh, S. (2012) Synthesis of 6″-triazole-substituted α-GalCer analogues as potent iNKT cell stimulating ligands. *Bioorg. Med. Chem.* 20, 7149−7154.

(11) Aspeslagh, S., Nemcovic, M., Pauwels, N., Venken, K., Wang, J., Van Calenbergh, S., Zajonc, D. M., and Elewaut, D. (2013) Enhanced TCR footprint by a novel glycolipid increases NKT-dependent tumor protection. *J. Immunol.* 191, 2916−2925.

(12) Birkholz, A., Nemcovic, M., Yu, E. D., Girardi, E., Wang, J., Khurana, A., Pauwels, N., Farber, E., Chitale, S., Franck, R. W., Tsuji, M., Howell, A., Van Calenbergh, S., Kronenberg, M., and Zajonc, D. M. (2015) α-Galactosylceramide Differently Influence Mouse and Human Type I Natural Killer T Cell Activation. *J. Biol. Chem.* 290, 17206−17217.

(13) Zhou, X.-T., Forestier, C., Goff, R. D., Li, C., Teyton, L., Bendelac, A., and Savage, P. B. (2002) Synthesis and NKT cell stimulating properties of fluorophore- and biotin-appended 6″-amino-6″-deoxy-galactosylceramides. *Org. Lett.* 4, 1267−1270.

(14) Trappeniers, M., Van Beneden, K., Decruy, T., Hillaert, U., Linclau, B., Elewaut, D., and Van Calenbergh, S. (2008) 6′-Derivatised α-GalCer analogues capable of inducing strong CD1d-mediated Th1-biased NKT cell responses in mice. *J. Am. Chem. Soc.* 130, 16468−16469.

(15) Tashiro, T., Nakagawa, R., Inoue, S., Shiozaki, M., Watarai, H., Taniguchi, M., and Mori, K. (2008) RCAI-61, the 6′-O-methylated analog of KRN7000: Its synthesis and potent bioactivity for mouse lymphocytes to produce interferon-gamma in vivo. *Tetrahedron Lett.* 49, 6827−6830.

(16) Pauwels, N., Aspeslagh, S., Vanhoenacker, G., Sandra, K., Yu, E. D., Zajonc, D. M., Elewaut, D., Linclau, B., and Van Calenbergh, S. (2011) Divergent synthetic approach to 6″-modified α-GalCer analogues. *Org. Biomol. Chem.* 9, 8413−8421.

(17) Hsieh, M.-H., Hung, J.-T., Liw, Y.-W., Lu, Y.-J., Wong, C.-H., Yu, A. L., and Liang, P.-H. (2012) Synthesis and evaluation of acyl-chain- and galactose-6″-modified analogues of α-GalCer for NKT cell activation. *ChemBioChem* 13, 1689–1697.

(18) Jervis, P. J., Graham, L. M., Foster, E. L., Cox, L. R., Porcelli, S. A., and Besra, G. S. (2012) New CD1d agonists: Synthesis and biological activity of 6″-triazole-substituted α-galactosyl ceramides. *Bioorg. Med. Chem. Lett.* 22, 4348–4352.

(19) Chennamadhavuni, D., Saavedra-Avila, N. A., Carreno, L. J., Guberman-Pfeffer, M. J., Arora, P., Yongqing, T., Pryce, R., Koay, H.-F., Godfrey, D. I., Keshipeddy, S., Richardson, S. K., Sundararaj, S., Lo, J. H., Wen, X., Gascon, J. A., Yuan, W., Rossjohn, J., Le Nours, J., Porcelli, S. A., and Howell, A. R. (2018) Dual modifications of α-galactosylceramide synergize to promote activation of human invariant natural killer T cells and stimulate anti-tumor immunity. *Cell Chem. Biol.* 25, 571–584 e578.

(20) Zajonc, D. M., Cantu, C., III, Mattner, J., Zhou, D., Savage, P. B., Bendelac, A., Wilson, I. A., and Teyton, L. (2005) Structure and function of a potent agonist for the semi-invariant natural killer T cell receptor. *Nat. Immunol.* 6, 810–818.

(21) Koch, M., Stronge, V. S, Shepherd, D., Gadola, S. D, Mathew, B., Ritter, G., Fersht, A. R, Besra, G. S, Schmidt, R. R, Jones, E Y., and Cerundolo, V. (2005) The crystal structure of human CD1d with and without α-galactosylceramide. *Nat. Immunol.* 6, 819–826.

(22) Borg, N. A., Wun, K. S., Kjer-Nielsen, L., Wilce, M. C. J., Pellicci, D. G., Koh, R., Besra, G. S., Bharadwaj, M., Godfrey, D. I., McCluskey, J., and Rossjohn, J. (2007) CD1d-lipid-antigen recognition by the semi-invariant NKT T-cell receptor. *Nature* 448, 44–49.

(23) Barbieri, L., Costantino, V., Fattorusso, E., Mangoni, A., Aru, E., Parapini, S., and Taramelli, D. (2004) Immunomodulatory α-galactoglycosphingolipids: Synthesis of a 2′-O-methyl-α-Gal-GSL and evaluation of its immunostimulating capacity. *Eur. J. Org. Chem.* 2004, 468–473.

(24) Wu, D., Xing, G.-W., Poles, M. A., Horowitz, A., Kinjo, Y., Sullivan, B., Bodmer-Narkevitch, V., Plettenburg, O., Kronenberg, M., Tsuji, M., Ho, D. D., and Wong, C.-H. (2005) Bacterial glycolipids and analogs as antigens for CD1d-restricted NKT cells. *Proc. Natl. Acad. Sci. U. S. A.* 102, 1351–1356.

(25) Raju, R., Castillo, B. F., Richardson, S. K., Thakur, M., Severins, R., Kronenberg, M., and Howell, A. R. (2009) Synthesis and evaluation of 3″- and 4″-deoxy and -fluoro analogs of the immunostimulatory glycolipid, KRN7000. *Bioorg. Med. Chem. Lett.* 19, 4122–4125.

(26) Xia, C., Zhang, W., Zhang, Y., Chen, W., Nadas, J., Severin, R., Woodward, R., Wang, B., Wang, X., Kronenberg, M., and Wang, P. G. (2009) The roles of 3′ and 4′ hydroxy groups in alpha-galactosylceramide stimulation of invariant natural killer T cells. *ChemMedChem* 4, 1810–1815.

(27) Zhang, W., Xia, C., Nadas, J., Chen, W., Gu, L., and Wang, P. G. (2011) Introduction of aromatic group on 4′-OH of α-GalCer manipulated NKT cell cytokine production. *Bioorg. Med. Chem.* 19, 2767–2776.

(28) Wu, T.-N., Lin, K.-H., Wu, Y.-T., Huang, J.-H., Hung, J.-T., Wu, J.-C., Chen, C.-Y., Chu, K.-C., Lin, N.-H., Yu, A. L., and Wong, C.-H. (2016) Phenyl glycolipids with different glycosyl groups exhibit differences in murine and human iNKT cell activation. *ACS Chem. Biol.* 11, 3431–3441.

(29) Janssens, J., Decruy, T., Venken, K., Seki, T., Krols, S., Van der Eycken, J., Tsuji, M., Elewaut, D., and Van Calenbergh, S. (2017) Efficient divergent synthesis of new immunostimulant 4″-modified α-galactosylceramide analogues. *ACS Med. Chem. Lett.* 8, 642–647.

(30) Janssens, J., Bitra, A., Wang, J., Decruy, T., Venken, K., van der Eycken, J., Elewaut, D., Zajonc, D. M., and van Calenbergh, S. (2019) 4″-O-Alkylated alpha-galactosylceramide analogues as iNKT-cell Antigens: Synthetic, biological, and structural studies. *ChemMedChem* 14, 147–168.

(31) Xia, C., Yao, Q., Schumann, J., Rossy, E., Chen, W., Zhu, L., Zhang, W., De Libero, G., and Wang, P. G. (2006) Synthesis and biological evaluation of α-galactosylceramide (KRN7000) and isoglobotrihexosylceramide (iGb3). *Bioorg. Med. Chem. Lett.* 16, 2195–2199.

(32) Bi, J., Wang, J., Zhou, K., Wang, Y., Fang, M., and Du, Y. (2015) Synthesis and biological activities of 5-thio- α-GalCers. *ACS Med. Chem. Lett.* 6, 476–480.

(33) Bricard, G., Venkataswamy, M. M., Yu, K. O. A., Im, J. S., Ndonye, R. M., Howell, A. R., Veerapen, N., Illarionov, P. A., Besra, G. S., Li, Q., Chang, Y.-T., and Porcelli, S. A. (2010) α-Galactosylceramide analogs with weak agonist activity for human iNKT cells define new candidate anti-inflammatory agents. *PLoS One* 5, e14374.

(34) Im, J. S., Arora, P., Bricard, G., Molano, A., Venkataswamy, M. M., Baine, I., Jerud, E. S., Goldberg, M. F., Baena, A., Yu, K. O. A., Ndonye, R. M., Howell, A. R., Yuan, W., Cresswell, P., Chang, Y.-T., Illarionov, P. A., Besra, G. S., and Porcelli, S. A. (2009) Kinetics and cellular site of glycolipid loading control the outcome of natural killer T cell activation. *Immunity* 30, 888–898.

(35) Wen, X., Rao, P., Carreno, L. J., Kim, S., Lawrenczyk, A., Porcelli, S. A., Cresswell, P., and Yuan, W. (2013) Human CD1d knock-in mouse model demonstrates potent anti-tumor potential of human CD1d-restricted invariant natural killer T cells. *Proc. Natl. Acad. Sci. U. S. A.* 110, 2963–2968.

(36) Arora, P., Baena, A., Yu, K. O. A., Saini, N. K., Kharkwal, S. S., Goldberg, M. F., Kunnath-Velayudhan, S., Carreno, L. J., Venkataswamy, M. M., Kim, J., Lazar-Molnar, E., Lauvau, G., Chang, Y.-t., Liu, Z., Bittman, R., Al-Shamkhani, A., Cox, L. R., Jervis, P. J., Veerapen, N., Besra, G. S., and Porcelli, S. A. (2014) A single subset of dendritic cells controls the cytokine bias of natural killer T cell responses to diverse glycolipid antigens. *Immunity* 40, 105–116.

(37) Godfrey, D. I., Le Nours, J., Andrews, D. M., Uldrich, A. P., and Rossjohn, J. (2018) Unconventional T cell targets for cancer immunotherapy. *Immunity* 48, 453–473.

(38) Lee, Y. J., Wang, H., Starrett, G. J., Phuong, V., Jameson, S. C., and Hogquist, K. A. (2015) Tissue-specific distribution of iNKT cells impacts their cytokine response. *Immunity* 43, 566–578.

(39) Arora, P., Venkataswamy, M. M., Baena, A., Bricard, G., Li, Q., Veerapen, N., Ndonye, R., Park, J.-J., Lee, J. H., Seo, K.-C., Howell, A. R., Chang, Y.-T., Illarionov, P. A., Besra, G. S., Chung, S.-K., and Porcelli, S. A. (2011) A rapid fluorescence-based assay for classification of iNKT cell activating glycolipids. *J. Am. Chem. Soc.* 133, 5198–5201.

(40) Spada, F. M., Koezuka, Y., and Porcelli, S. A. (1998) CD1d-Restricted recognition of synthetic glycolipid antigens by human natural killer T cells. *J. Exp. Med.* 188, 1529–1534.

(41) Madhavi Sastry, G., Adzhigirey, M., Day, T., Annabhimoju, R., and Sherman, W. (2013) Protein and ligand preparation: Parameters, protocols, and influence on virtual screening enrichments. *J. Comput.-Aided Mol. Des.* 27, 221–234.

(42) Friesner, R. A., Banks, J. L., Murphy, R. B., Halgren, T. A., Klicic, J. J., Mainz, D. T., Repasky, M. P., Knoll, E. H., Shelley, M., Perry, J. K., Shaw, D. E., Francis, P., and Shenkin, P. S. (2004) Glide: a new approach for rapid, accurate docking and scoring. 1. Method and assessment of docking accuracy. *J. Med. Chem.* 47, 1739–1749.

(43) Bowers, K. J., Chow, E., Xu, H., Dror, R. O., Eastwood, M. P., Gregersen, B. A., Klepeis, J. L., Kolossvary, I., Moraes, M. A., Sacerdoti, F. D., Salmon, J. K., Shan, Y., and Shaw, D. E. (2006) Scalable algorithms for molecular dynamics simulations on commodity clusters. Proceedings of the 2006 ACM/IEEE conference on supercomputing, Tampa, Florida.